JOURNAL OF MATERIALS SCIENCE 31 (1996) 387–397

Age hardening and precipitation in a cast magnesium–rare-earth alloy

L.Y. WEI
Department of Engineering Materials, Luleå University of Technology, S 971 87 Luleå, Sweden

G.L. DUNLOP
CRC for Alloy and Solidification Technology (CAST), Department of Mining and Metallurgical Engineering, The University of Queensland, Queensland 4072, Australia

H. WESTENGEN
Norsk Hydro a.s., Research Centre Porsgrunn, P.O. Box 2560, N-3901 Porsgrunn, Norway

The precipitation sequence responsible for the age-hardening behaviour of a cast Mg–1.3 wt% rare-earth alloy has been investigated by analytical electron microscopy. Very fine intermediate precipitates formed at an early stage of ageing. Plate-shaped Mg_3MM β′ precipitates (MM = misch metal) and hexagonal prism-shaped $Mg_{12}MM$ β precipitates were primarily responsible for age hardening. Precipitate morphologies, crystal structures and crystallographic orientation relationship were determined for the various types of precipitates that formed during ageing at different temperatures.

1. Introduction

The sharp decrease in the solubility of rare-earth elements in magnesium alloys with decreasing temperature offers the possibility of age hardening. Materials of this type containing grain-refining additions of zirconium exhibit high strength and good high-temperature creep resistance [1]. The present paper is concerned with the detailed characteristics of the precipitation sequence responsible for the age-hardening behaviour of a cast Mg–1.3 wt % rare-earth (RE) alloy in which the rare-earth additions were made in the form of misch metal. The investigation, which used analytical electron microscopy, concentrated upon the morphologies, crystal structures and crystallographic orientation relationships for the different types of precipitate that formed in this alloy.

Previous work on precipitation in a Mg–Nd alloy [2, 3] suggested the ageing sequence to be supersaturated solid solution → Guinier–Preston zones → β″ → β′ → β. Needle-shaped Guinier–Preston (GP) zones formed at temperatures between room temperature and 170 °C. The β″ precipitates formed in the temperature range 200–260 °C and these had a perfectly coherent DO_{19} hexagonal structure with $a = 2a_{Mg}$, $c = c_{Mg}$. Pike and Noble suggested that the

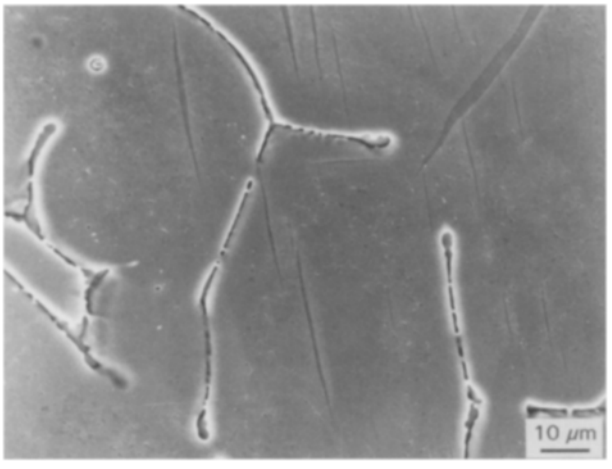

Figure 1 Microstructure of the Mg–1.3RE alloy in the as-cast condition. The interdendritic phase was $Mg_{12}MM$. SEM.

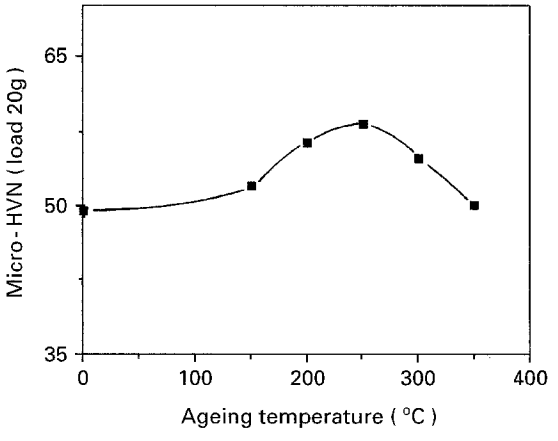

Figure 2 The age-hardening response of the Mg–1.3RE alloy following ageing for 3 h at different temperatures.

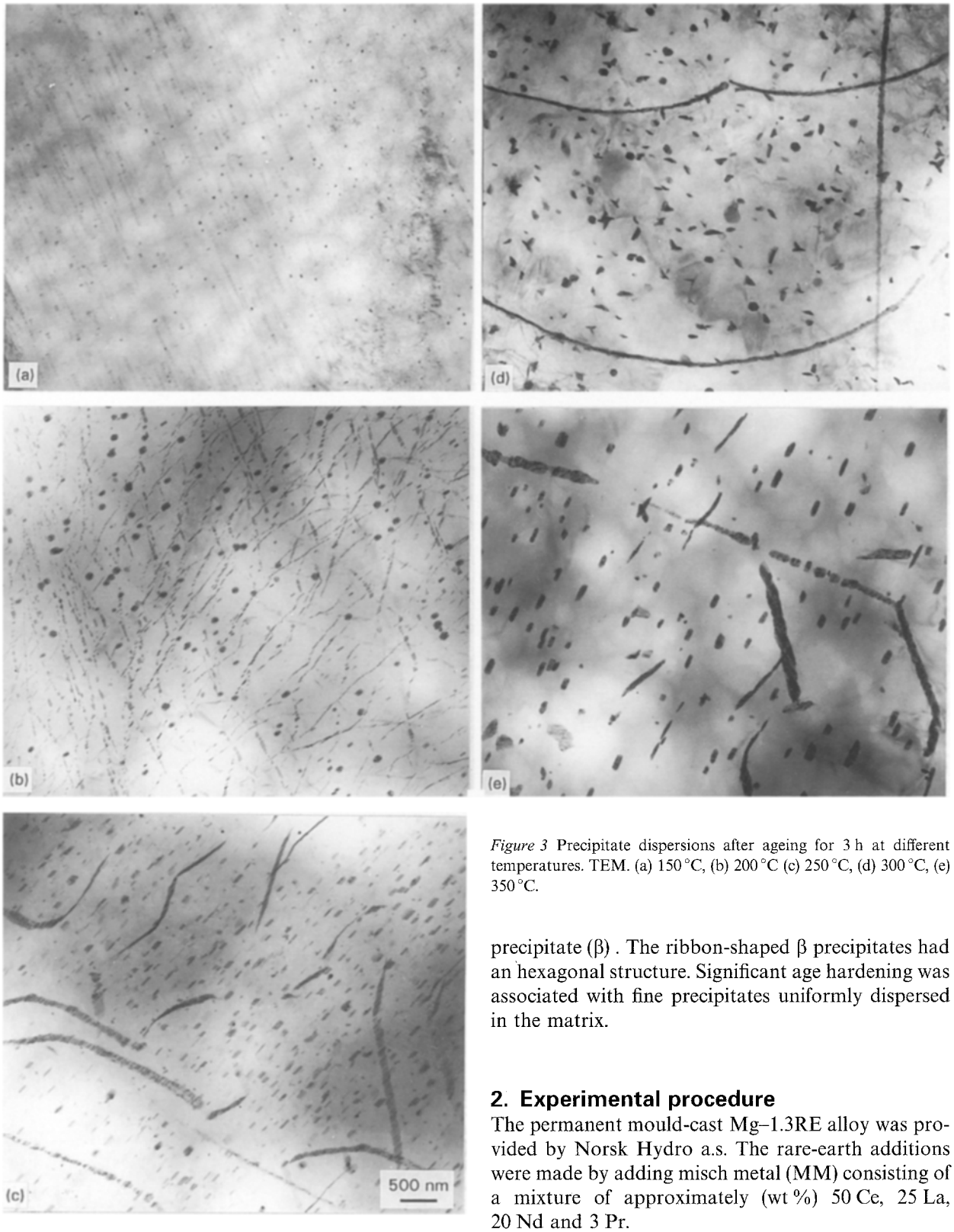

Figure 3 Precipitate dispersions after ageing for 3 h at different temperatures. TEM. (a) 150 °C, (b) 200 °C (c) 250 °C, (d) 300 °C, (e) 350 °C.

structure of β′ was possibly hexagonal with $a = 0.52$ nm, $c = 1.3$ nm [2]. However, Karimzadeh [3] and Gradwell [4] indicated that β′ had an fcc structure with $a = 0.735$ nm and a composition close to Mg_2Nd_{17}. The β phase has an incoherent bct structure with $a = 1.031$ nm, $c = 0.593$ nm and a composition corresponding to $Mg_{12}Nd$.

Omori *et al.* [5, 6] found that the precipitation sequence in a Mg–1.3Ce alloy was supersaturated solid solution → intermediate precipitate → equilibrium precipitate (β) . The ribbon-shaped β precipitates had an hexagonal structure. Significant age hardening was associated with fine precipitates uniformly dispersed in the matrix.

2. Experimental procedure

The permanent mould-cast Mg–1.3RE alloy was provided by Norsk Hydro a.s. The rare-earth additions were made by adding misch metal (MM) consisting of a mixture of approximately (wt %) 50 Ce, 25 La, 20 Nd and 3 Pr.

Specimens for heat treatment were solution treated for 2 h at 550 °C followed by a water quench. During solution treatment, the specimens were sealed in vacuum in Pyrex capsules. Subsequent ageing was carried out at temperature ranges between 150 and 350 °C for 3 h. During the ageing treatment, the specimens were embedded in MgO powder in order to avoid burning and severe oxidation.

Microhardness measurements using a load of 20 g were carried out on the aged specimens. Thin foil specimens for transmission electron microscopy were

prepared by electropolishing in an electrolyte of 1/3 nitric acid in ethanol and finally ion-beam thinning at a voltage of 2.7 keV and incident angle of 15°. They were examined in Jeol 2000 FX TEM/STEM and Jeol 733 SEM instruments.

3. Results

3.1. The microstructure of the as-cast and solution-treated alloy

The as-cast Mg–1.3 RE alloy had a dendritic cast structure. The coarse intergranular phase, shown in Fig. 1, was identified as $Mg_{12}MM$ which has a crystal structure similar to $CeMg_{12}$ and contained a variety of rare-earth elements from the misch metal. The dendrites were fairly inhomogeneous and some coarse precipitation occurred within them after solidification had taken place. A number of lenticular twins was present in the dendrite matrix. Selected-area diffraction showed that the twins formed on (1 0 2) planes and that the hexagonal axes ([0 0 1]) of the twinned crystals were nearly perpendicular (86.3 °C) to each other. Most of the intergranular $Mg_{12}MM$ spheroidized into relatively small particles during solution

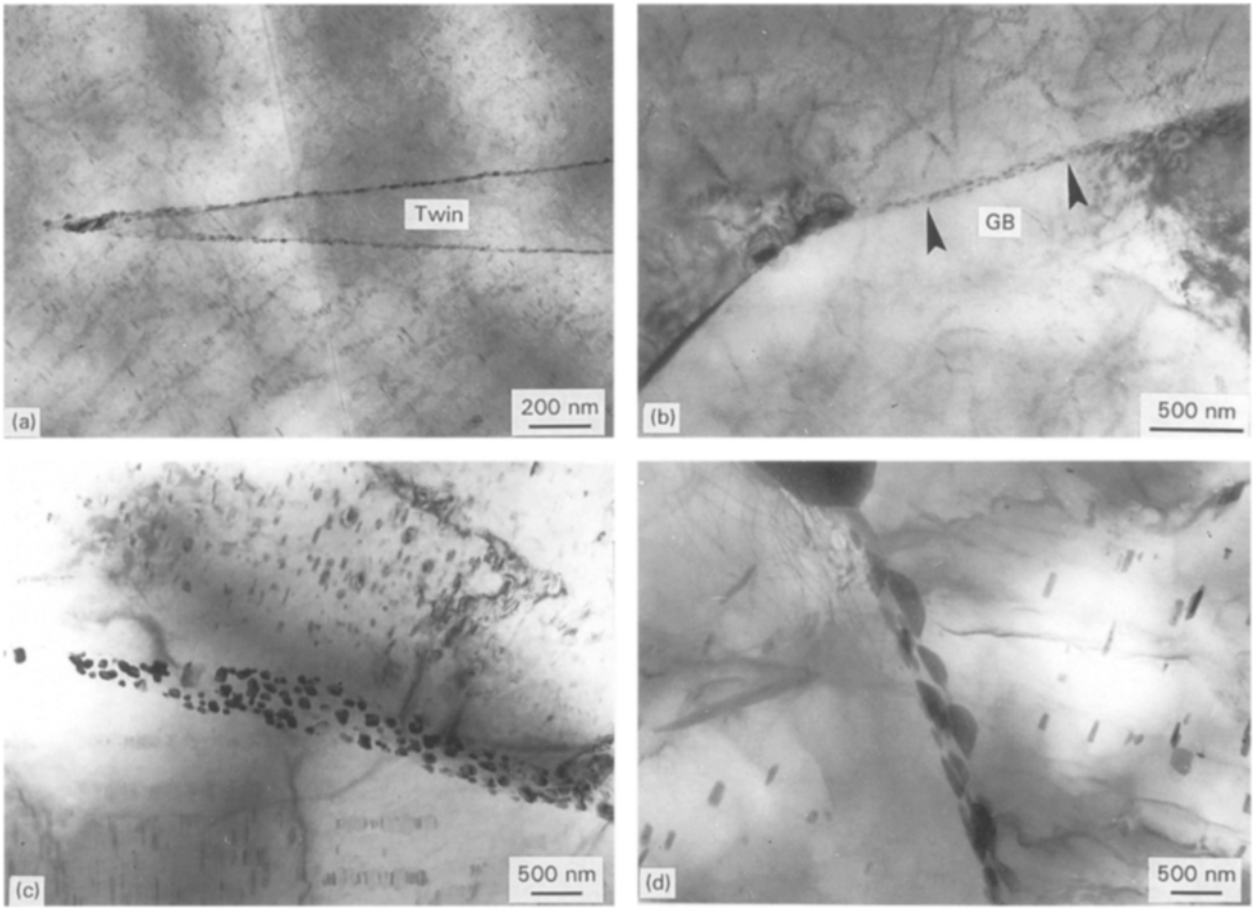

Figure 4 Precipitation on grain (GB) and twin boundaries in specimens aged for 3 h. TEM. (a) Twin boundary, after ageing at 150° C; (b) grain boundary after ageing at 150 °C; (c) aged at 250 °C; (d) aged at 350 °C.

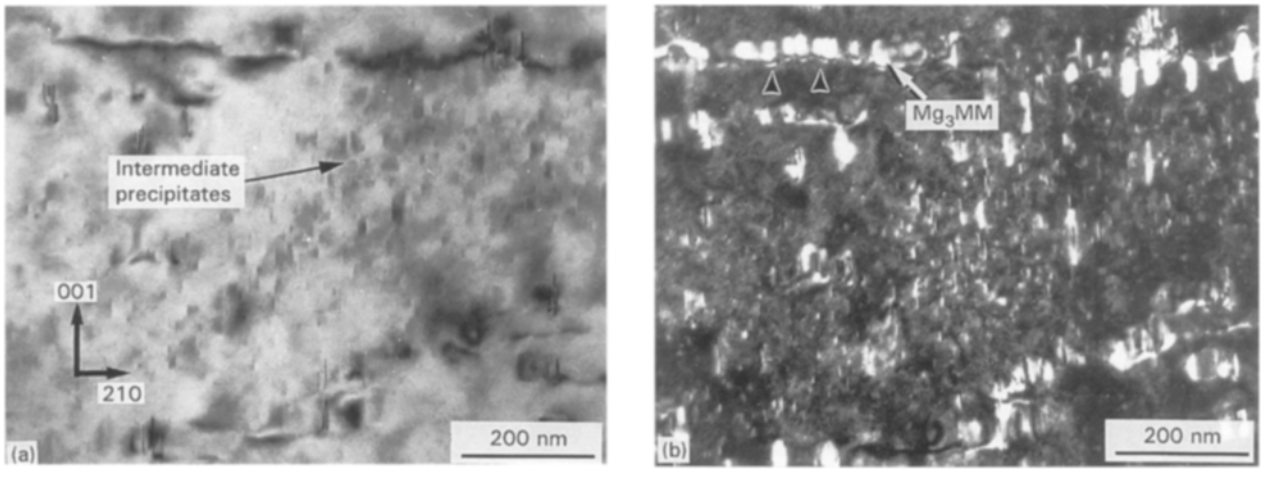

Figure 5 The early stages of precipitation after ageing 3 h at 150 °C. TEM. (a) Bright field showing a uniform dispersion of fine intermediate precipitates; (b) weak-beam dark-field, using a $(2\,0\,1)_{Mg}$ reflection beam, showing Mg_3MM precipitates formed on dislocations (arrowed).

treatment with some partial dissolution. Precipitates dispersed within the α(Mg) grains of the as-cast alloy dissolved during solution treatment.

3.2. Age-hardening and precipitation behaviour during isochronal ageing treatments

3.2.1. Micro-hardness and precipitate dispersions of specimens aged for 3 h at different temperatures

The results of micro-hardness measurements made within the dendrites of aged specimens that had been aged for 3 h are shown in Fig. 2. Peak hardness occurred between 200 and 250 °C with overageing occurring at higher temperatures.

Transmission electron micrographs from specimens aged for 3 h at different temperatures are shown in Fig. 3. Two types of precipitate morphology developed in these specimens. One of them had a granular shape and the other one was ribbon-like. The microstructure corresponding to peak hardness, shown in Fig. 3b and c, had a relatively large proportion of the ribbon-shaped precipitates. Softening in association with overageing was accompanied by a decrease in the amount of ribbon precipitate and coarsening of both granular and ribbon precipitates. The details of these two types of precipitates, including their morphologies, crystal structures, orientation relationships with the matrix and phase transformations will be discussed below.

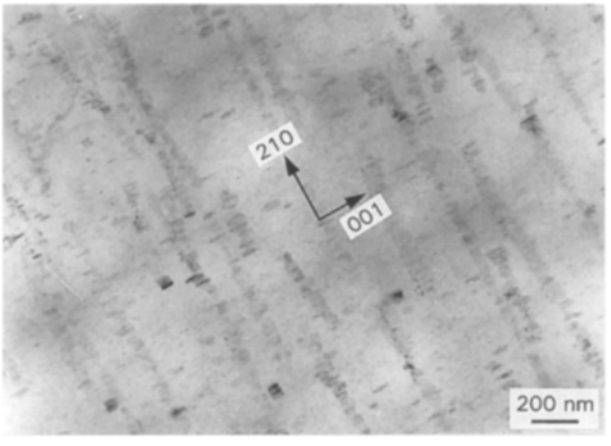

Figure 6 Ribbon precipitates of Mg_3MM after ageing 3 h at 150 °C. TEM.

3.2.2. Precipitation on twin and grain boundaries

After ageing for 3 h at temperatures as low as 150 °C, precipitates with a granular shape had formed preferentially at grain boundaries and twin boundaries (Fig. 4a and b). These granular particles were identified as the equilibrium $Mg_{12}MM$ β phase, whereas ribbon-shaped precipitates dispersed uniformly within α(Mg) matrix were another intermediate precipitate. As shown in Fig. 4c and d, the intergranular β particles coarsened substantially with increasing ageing temperature. The average particle sizes (in diameter) for these precipitates were about 20, 120 and 300 nm for specimens aged at 150, 250 and 350 °C, respectively.

3.2.3. The early stages of precipitation within the matrix and the formation of Mg_3MM β′ precipitates

The transmission electron micrographs in Fig. 5a and b, taken close to two beam conditions, show strain contrast from fine precipitates dispersed homogeneously in the matrix of a specimen that had been aged for 3 h at 150 °C. These precipitates lay in $(1\,0\,0)_{Mg}$ planes and had $[0\,0\,1]_{Mg}$ growth directions. The inter-precipitate spacing was about 15 nm. The structure of these very fine precipitates has not yet been determined. They seem to be an intermediate precipitate and did not appear at higher ageing temperatures. The weak-beam dark-field image in Fig. 5b shows the strain contrast arising from the early stage of precipitation and shows some other type of precipitate forming on dislocations. The image in Fig. 6 shows that this type of precipitate was ribbon-shaped with

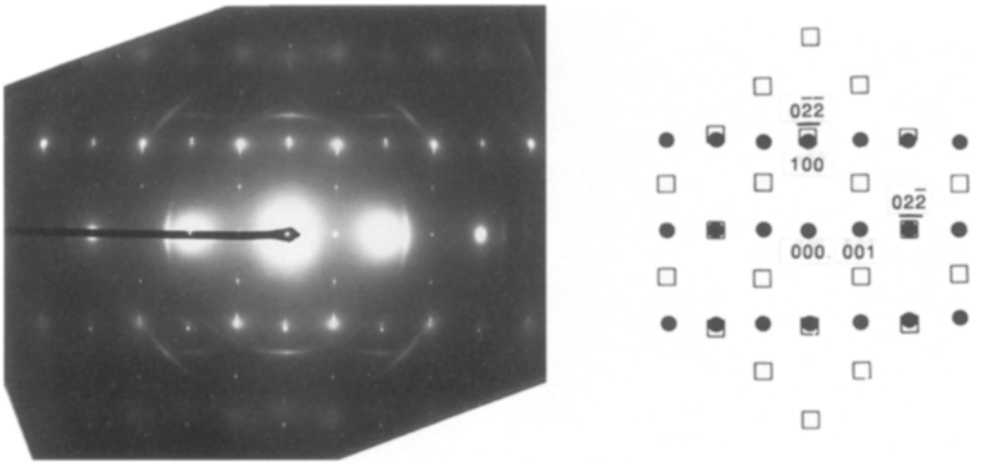

Figure 7 SAED pattern with $[0\,1\,0]_{Mg}$ zone axis of β′ precipitate dispersion after ageing 3 h at 150 °C. (●) α-Mg, with [0 1 0] zone axis; (□) β′ precipitate with [1 0 0] zone axis.

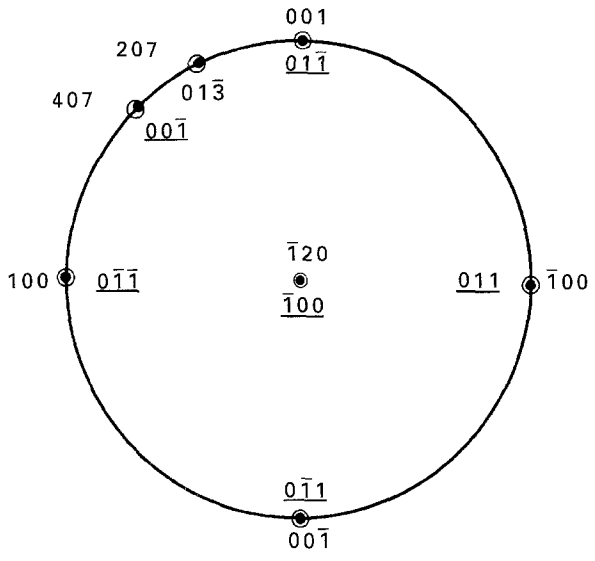

Figure 8 Stereographic projection illustrating the orientation relationship between the α(Mg) matrix and β′Mg_3MM precipitates: $(0\,0\,1)_{Mg} \parallel (0\,1\,\bar{1})_{\beta'}$, $(1\,0\,0)_{Mg} \parallel (0\,\bar{1}\,\bar{1})_{\beta'}$, $(\bar{1}\,2\,0)_{Mg} \parallel (\bar{1}\,0\,0)_{\beta'}$. (●) Mg_3MM precipitate: cubic [$\bar{1}$00] axis; (○) α-Mg matrix: hcp [010] axis, axial ratio = 1.623.

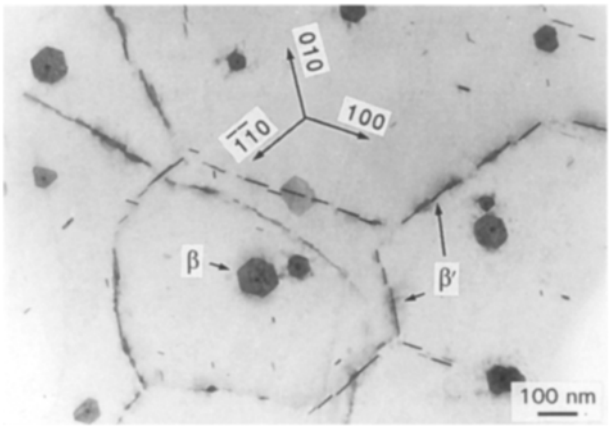

Figure 9 Precipitation of both β′ platelets and β phase after ageing 3 h at 200 °C. Note the dark contrast nucleus of the β precipitates. TEM, foil plane parallel to $(0\,0\,1)_{Mg}$.

a growth direction of $[0\,0\,1]_{Mg}$. Selected-area electron diffraction confirmed that these precipitate ribbons were the Mg_3MM β′ phase. The crystal structure of the β′ phase was confirmed as fcc with the lattice parameter $a \approx 0.735$ nm. This is the same as the structure of Mg_3Ce (fcc, a = 0.7428 nm) [7] but here it is designated as Mg_3MM, because a number of different rare-earth elements were detected in it by EDX/STEM. The crystallographic orientation relationship between the β′ phase and the matrix was determined from a series of diffraction patterns. Such as that shown in Fig. 7, This orientation relationship was established to be

$$(0\,0\,1)_{Mg} \parallel (0\,1\,\bar{1})_{\beta'}$$

$$(1\,0\,0)_{Mg} \parallel (0\,\bar{1}\,\bar{1})_{\beta'}$$

$$(\bar{1}\,2\,0)_{Mg} \parallel (\bar{1}\,0\,0)_{\beta'}$$

This orientation relationship is shown in the stereographic projection of Fig. 8.

The β′ precipitates were also present after ageing at 200 °C and developed a plate-like morphology with a $\{1\,0\,0\}_{Mg}$ habit plane. The precipitates obeying all three variants of the foregoing orientation relationship can be clearly seen in Fig. 9. The three-fold multiplicity of the orientation relationship results from the six-fold rotation symmetry of the matrix and the three-fold symmetry of the β′ phase, and from the fact that their rotation axes are parallel.

The morphology of the β′ precipitates after ageing at 200 °C is further illustrated by Fig. 10. The foil plane in Fig. 10a was close to $(0\,0\,1)_{Mg}$ and in this orientation the β′ precipitates appear as rods. The two-dimensional plate morphology of these precipitates was revealed by tilting ~48° around the direction shown by the arrow, **R**, in Fig. 10a. As shown in Fig. 10b, the β′ precipitates then appeared as platelets arranged along dislocations to give a ribbon-like appearance. The fact that these precipitates had formed on dislocations is shown clearly by the weak-beam image in Fig. 11.

The habit planes of the β′ precipitates were found to be consistent with the prism planes of the magnesium

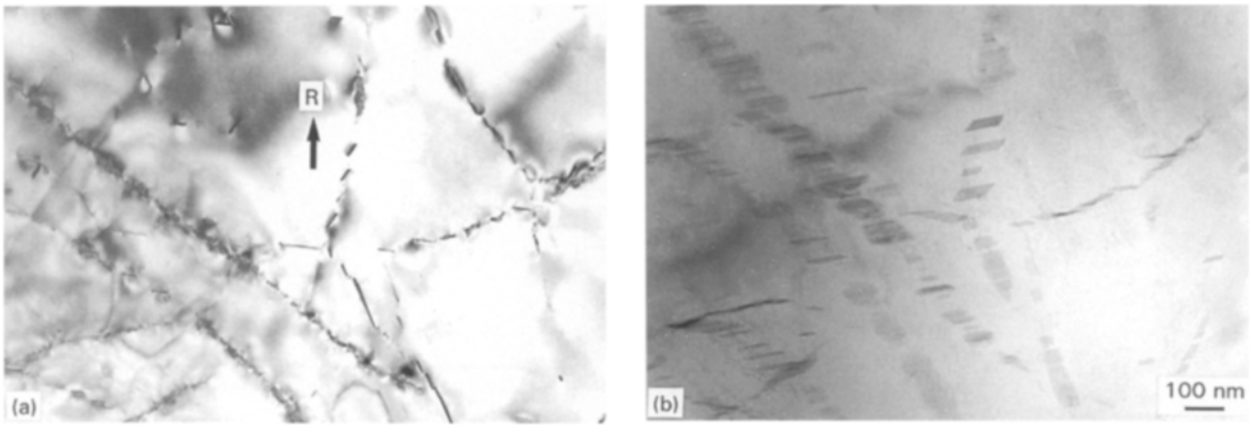

Figure 10 The plate-like morphology of β′ precipitates. TEM. (a) β′ precipitated on dislocation; foil normal close to [0 0 1] Mg; (b) the same area as (a) after tilting about 48° about the axis. **R**

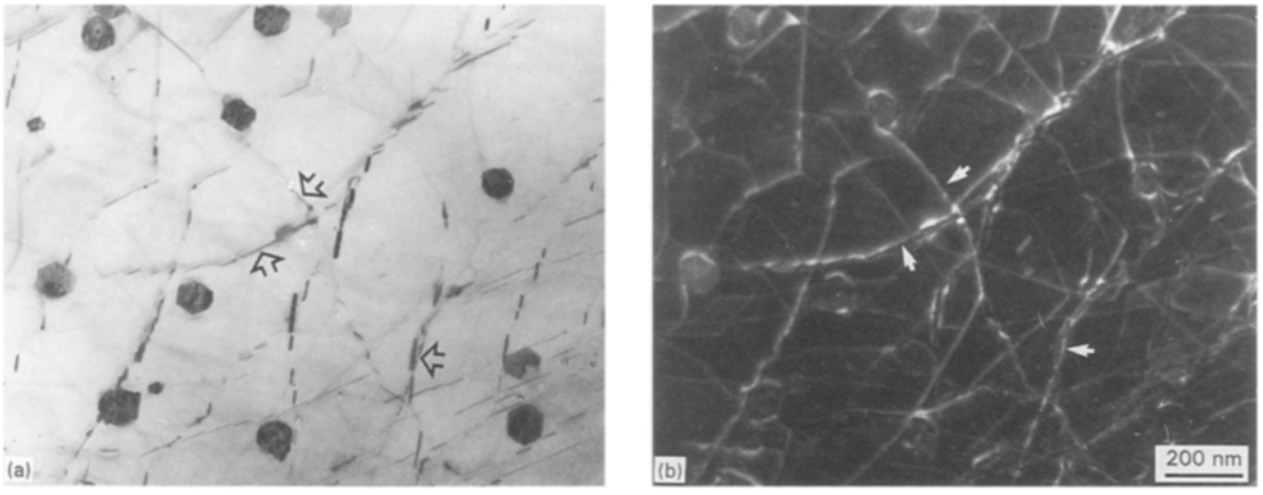

Figure 11 Precipitation of β′ on dislocations. Note also the β precipitates with the dark-contrast nuclei. Aged 3 h at 200 °C. TEM. (a) Bright field, (b) weak-beam dark-field using a $(\bar{2}\,1\,0)_{Mg}$ diffracted beam.

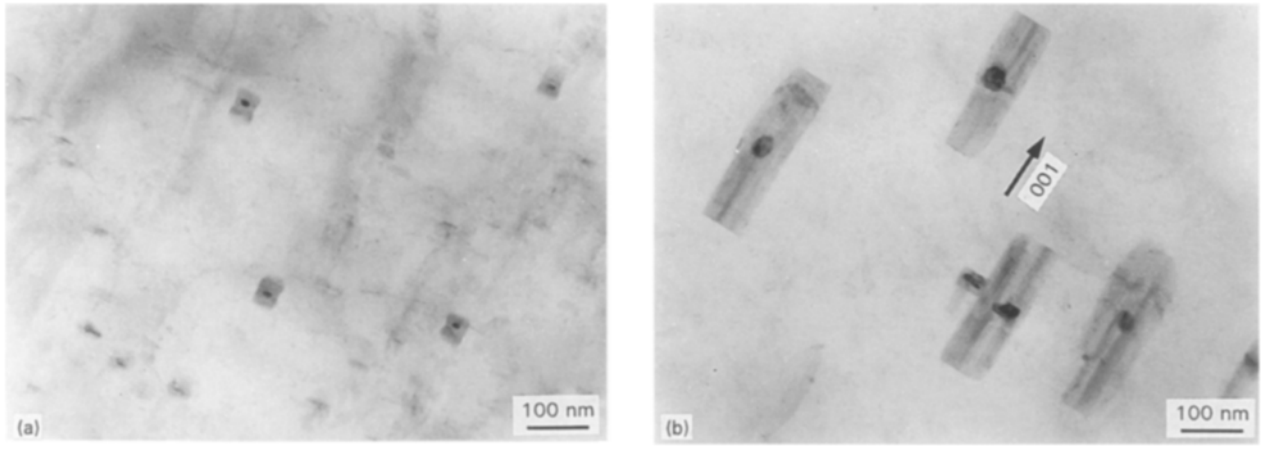

Figure 12. Precipitation of β phase. TEM. Foil normal close to $[2\,1\,0]_{Mg}$, (a) aged 3 h at 150 °C, (b) aged 3 h at 300 °C.

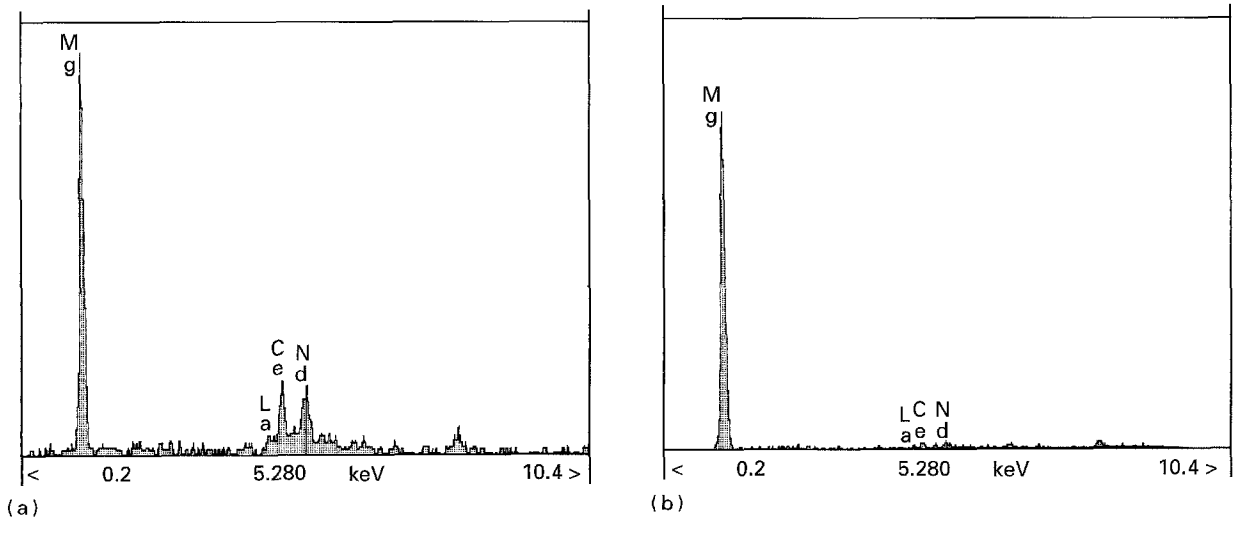

Figure 13 STEM/EDX spectra from a β precipitate, (a) from the dark-contrast nucleus, (b) from the outer-most part of the β precipitate.

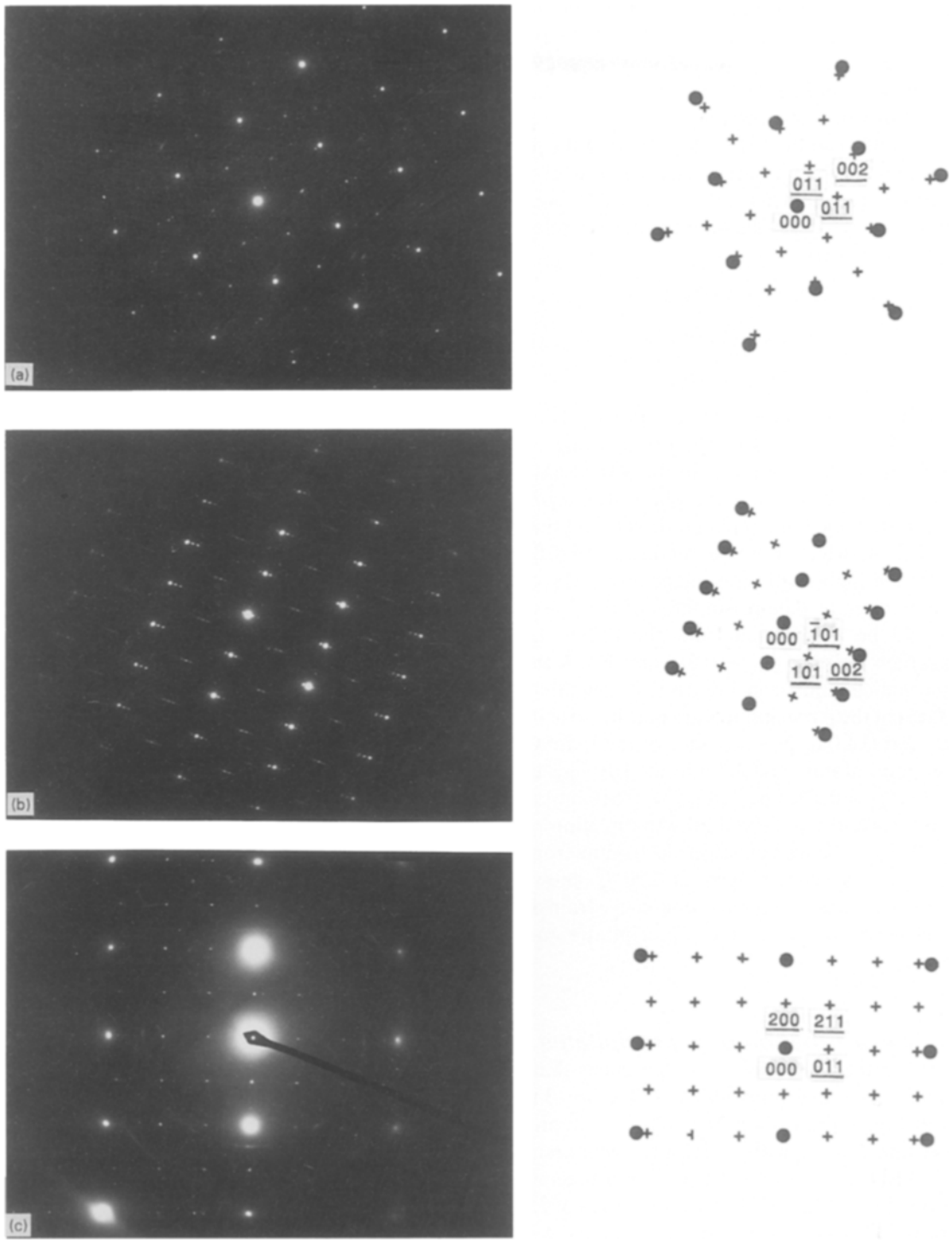

Figure 14 SAED patterns from β precipitates with schematic solutions (a) with $[0\,0\,1]_{Mg}/[1\,0\,0]_{\beta}$ zone axis, (b) with $[0\,\bar{1}\,0]_{Mg}/[0\,\bar{1}\,0]_{\beta}$ zone axis, (c) with $[2\,1\,0]_{Mg}/[0\,\bar{1}\,1]_{\beta}$ zone axis. (●) α-Mg, (+) β-precipitate.

matrix. High coherency existed at the interface, between β′ precipitates and the matrix, which was parallel to $\{1\,0\,0\}_{Mg}$ planes. There was only a small mismatch in the $[0\,0\,1]_{Mg}$ direction, where $d_{0\,0\,1_{Mg}} = 0.520\,\text{nm} \simeq d_{0\,1\,\bar{1}_{\beta'}}$.

3.2.4. β precipitates with hexagonal prism morphology

A third type of precipitate that formed in specimens, that had been age-hardened, was identified as β-phase. As shown in Fig. 9, these precipitates had a hexagonal shape when viewed in an $[0\,0\,1]_{Mg}$ beam direction and had apparently formed around a small (10–15 nm) inclusion that generally exhibited darker contrast than the surrounding precipitate. With other beam directions (Fig. 12) it could be seen that these precipitates had the morphology of a hexagonal prism. With increasing ageing temperatures the β precipitates grew mainly in the $[0\,0\,1]_{Mg}$ direction. Average prism heights increased from 35 nm to 250 nm and diameters from 50 nm to 100 nm when the temperature of ageing was increased from 150 °C to 300 °C.

The two STEM/EDX spectra in Fig. 13a and b were taken from the centre (nucleus) and outer-most part of a β precipitate. The nucleus had a much higher

content of rare-earth elements than the remainder of the precipitate. The measured increased rare-earth content of the nucleus is consistent with its darker contrast which can be concluded to be due to heavy-element absorption of electrons.

It was established by SAED (Fig. 14) that the β precipitates had the bct crystal structure of $Mg_{12}MM$ with lattice parameters $a \approx 1.03$ nm; $c \approx 0.60$ nm. The precipitates obeyed the following orientation relationship with the matrix

$$(1\,0\,0)_\beta \parallel (0\,0\,1)_{Mg}$$
$$(0\,1\,1)_\beta \parallel (\bar{1}\,2\,0)_{Mg}$$
$$(0\,\bar{1}\,1)_\beta \parallel (1\,1\,0)_{Mg}$$

This orientation relationship is illustrated by the stereographic project in Fig. 15. The splitting of the basic reflections of the β phase in the SAED patterns (see Fig. 14b) indicates that the phase was probably modulated by some kind of planar defects and that the planes of these defects were perpendicular to $(0\,0\,1)_{Mg}$.

Fig. 16 is a high-resolution image of an $Mg_{12}MM$ β-phase precipitate. The prism faces of the β precipitates could be determined from the $(0\,2\,0)_\beta$ lattice fringes which have $d_{(0\,2\,0)_\beta} = 0.516$ nm. From the directional indices shown in Fig. 16 it is clear that the prism faces of the β precipitates are parallel to $(1\,0\,0)_{Mg}$, $(0\,1\,0)_{Mg}$ and $(1\,\bar{1}\,0)_{Mg}$ prism planes of the matrix. Because of good atomic matching in the $[0\,0\,1]_{Mg}$ direction ($d_{0\,0\,1_{Mg}} = 0.520$ nm, $d_{2\,0\,0_\beta} = 0.516$ nm), the β precipitates had a preferred growth direction parallel to $[0\,0\,1]_{Mg}$. The transmission electron micrograph taken from a specimen aged at 200 °C shown in Fig. 17 reveals contrast due to coherency strain at the interfaces between both β′ and β precipitates and the matrix.

3.2.5. Transformation of β′ precipitates to β

No β′ precipitates were found in specimens that had been aged at temperatures above 250 °C for 3 h. As shown in Fig. 3, the ribbon-like chains of β′ precipitates became coarser with increasing ageing temperatures. SAED showed that the β′ ribbon precipitates transformed to β $Mg_{12}MM$ at temperatures of 250 °C and above. This type of β precipitate had the same orientation relationship with the matrix as the hexagonal prism β precipitates. However, they had an irregular morphology and lacked a high degree of coherency with the matrix. Thus specimens aged at temperatures higher than 250 °C contained two types of β precipitates. One of these formed at an early stage of ageing and had a high rare-earth content at their centres and the other had transformed from β′ precipitates at temperatures higher than 200 °C.

4. Discussion

4.1. Heterogeneous nucleation

Except for the very fine precipitate observed in specimens aged at 150 °C, most of the precipitates that formed during ageing of the Mg–1.3RE alloy nucleated heterogeneously. Precipitates were found to

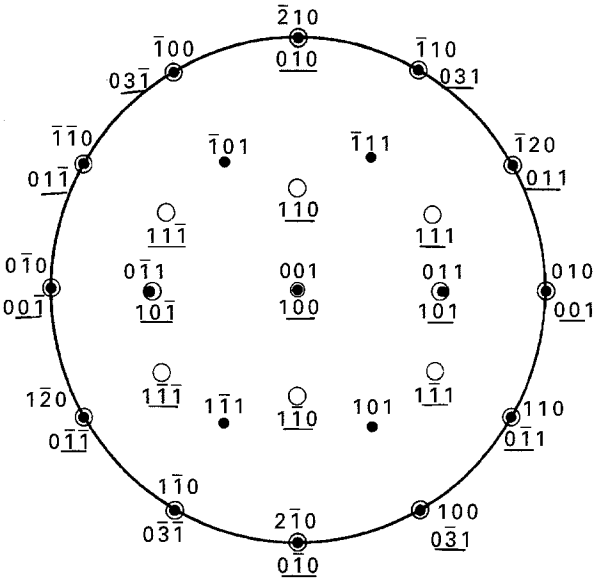

Figure 15 Stereographic projection illustrating the orientation relationship between β precipitates and the matrix. (●) α-Mg matrix, hcp [0 0 1] axis, axial ratio = 1.623; (○) $Mg_{12}MM$ β precipitate, bct, [1 0 0] axis, axial ratio = 0.577.

nucleate at grain and twin boundaries, on dislocations, and around some particles with high rare-earth contents.

For example, twins were found to form on (1 0 2) planes in the investigated alloy. The two hexagonal axes of the twinned crystals were nearly perpendicular to one another with the actual angle being 86.3°. According to Hume-Rothery *et al.* [8], it is not possible for the two halves of (1 0 2) twin crystals in a cph structure to fit together without some distortion of the lattice in the region of the boundary. This explains why β-phase precipitates can form at temperatures as low as 150 °C at twin boundaries because these sites have a large amount of elastic strain associated with them and this can reduce the nucleation barrier for precipitation.

The β phase precipitates with hexagonal prism morphology, had not been observed in previous work. The pre-existing rare-earth-rich inclusions that served as nuclei probably formed in the melt. These inclusions had not dissolved during the solution treatment at 550 °C for 2 h and offered high-energy sites for heterogeneous nucleation.

4.2. Precipitation sequence

The sequence of precipitation in the Mg–1.3RE alloy was established to be

supersaturated solution → fine intermediate precipitates → β′ (formed on dislocations) → β,
supersaturated solution → β (formed around the high RE inclusions).

The fine intermediate precipitates have yet to be characterized properly but it seems unlikely that they are GP zones as suggested by Pike and Noble [2] and

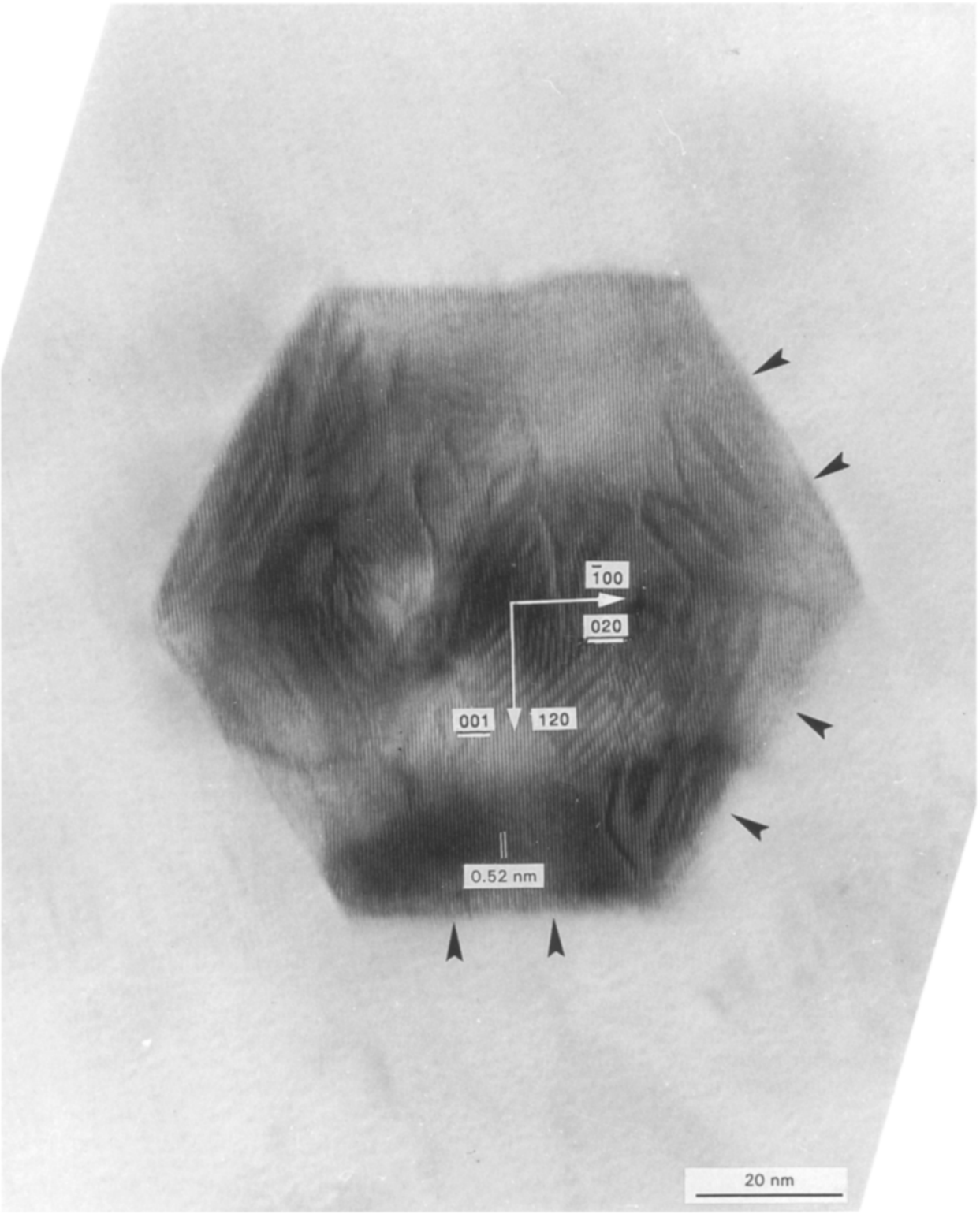

Figure 16 HREM image of a β Mg_{12}MM precipitate. Directional indices of the β precipitate are indicated with a bar underneath. Prism planes of the magnesium lattice are arrowed.

Karimzadeh [3] for Mg–Nd alloys. β′ precipitates with the crystal structure of Mg_3MM were found in the same specimen.

β′ precipitates were found in specimens after ageing at 150 and 200 °C, but not in specimens aged at 250 °C. The β′ precipitates transformed to thermodynamically stable Mg_{12}MM β precipitates at temperatures higher than 250° C. With reference to the binary Mg–Ce phase diagram [9], it can be deduced that the Mg_{12}MM phase is an equilibrium phase in this alloy.

Consistent with the work of Karimzadeh [3], the β′ precipitates were determined to have the same f c c crystal structure as $CeMg_3$ with $a \approx 0.735$ nm.

The equilibrium β precipitates arranged in irregular ribbons that formed at temperatures higher than 250 °C were determined to be the Mg_{12}MM phase, and it should be noted that the structure for β phase previously published by Omori *et al.* [5] is not correct.

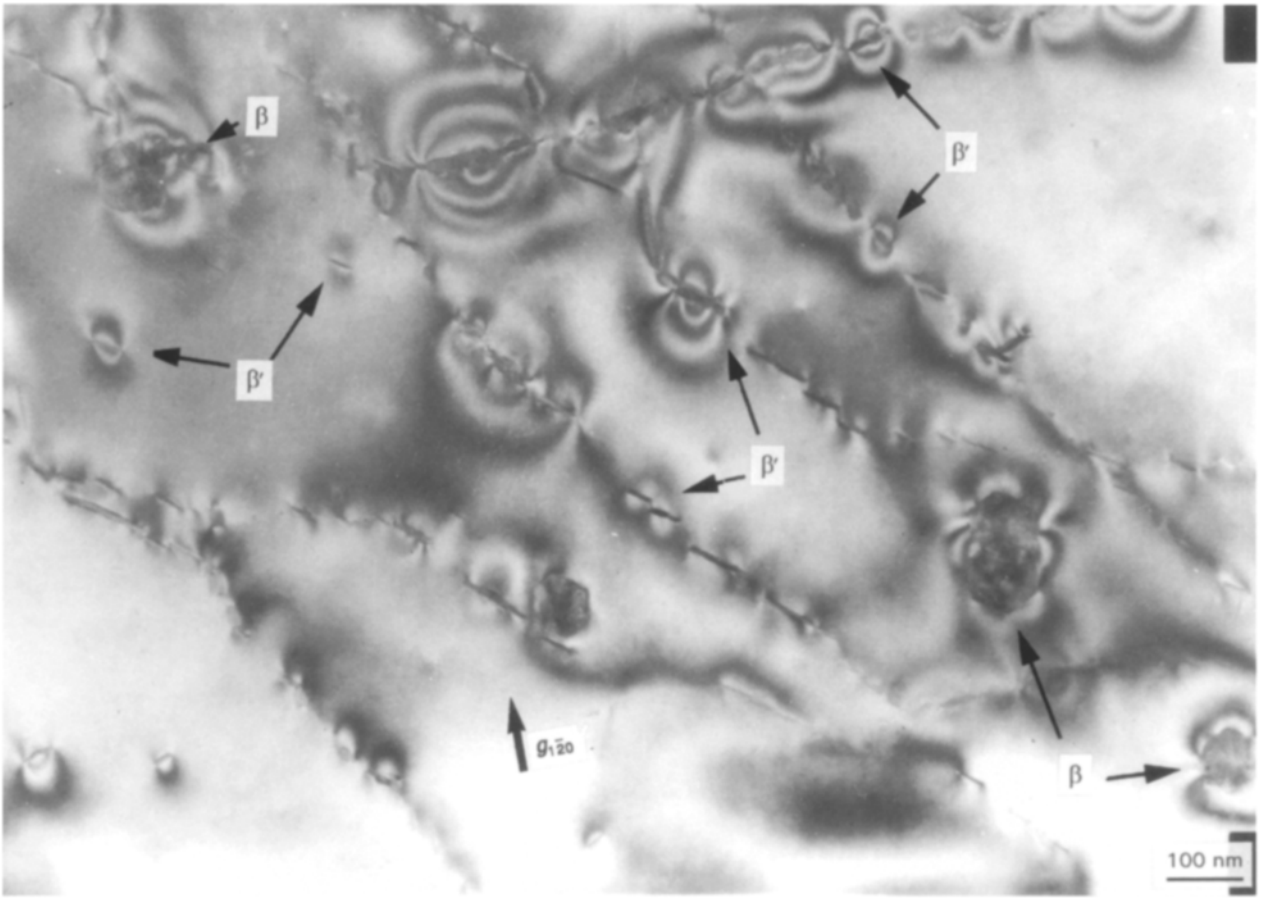

Figure 17 Coherency strain contrast from β′ and β precipitates after ageing 3 h at 200 °C. TEM. Two-beam condition, $g = 1\bar{2}0$.

The SAED patterns of β phase that were obtained here showed that this phase has a b c t structure.

The β′ plate-shaped intermetallic precipitates and the finely dispersed β hexagonal prism-shaped equilibrium precipitates were probably the main cause of hardening in this alloy, because both of these precipitates offer obstruction to basal slip within the α(Mg) matrix. With increasing ageing temperatures above 250 °C, the β′ precipitates transformed to the stable β phase and the coarsening of both morphologies of β precipitate lead to overageing.

5. Conclusions

1. The precipitation sequence during age hardening of the Mg–1.3RE alloy was

supersaturated solution → fine intermediate precipitates → β′ (formed on dislocations) → β,

supersaturated solution → β (formed around the high RE inclusions).

2. The plate-shaped β′ precipitates and the finely dispersed β hexagonal prism-shaped equilibrium precipitates were primarily responsible for age hardening. The onset of overageing coincided with transformation of β′ ribbon precipitates to β phase and coarsening of both morphologies of β precipitate.

3. Grain and twin boundaries were preferential sites for nucleation of β precipitates. The stable β phase first formed at these sites during ageing at 150 °C.

4. Fine intermediate precipitates formed on $(1\,0\,0)_{Mg}$ planes with $[0\,0\,1]_{Mg}$ growth directions. They were uniformly dispersed in the matrix of specimens aged at 150 °C together with fine β′ precipitates that had nucleated on dislocations.

5. The plate-shaped β′ precipitates were identified to be Mg_3MM with the same crystal structure as $CeMg_3$. The β′ plates lie on $\{1\,0\,0\}_{Mg}$ habit planes with high coherency with the matrix in $[0\,0\,1]_{Mg}$ directions.

6. Pre-existing high rare-earth content inclusions were efficient nucleation sites for finely dispersed β precipitates that formed at temperatures as low as 150 °C. These β precipitates had a hexagonal prism morphology with their prism faces parallel to $\{1\,0\,0\}_{Mg}$ prism planes of the matrix. The β precipitates were thermally stable up to 350 °C, but considerable coarsening occurred at these higher ageing temperatures.

7. The β′ precipitates were unstable at temperatures higher than 250 °C where they transformed to β phase.

Acknowledgements

The experimental work was carried out at Chalmers University of Technology and financial support was received from the Swedish Board for Technical Development and Norsk Hydro a.s.

References

1. A.J. MURPHY and R.J.M. PAYNE, *J. Inst. Metals.* **73** (1947) 105.
2. T.J. PIKE and B. NOBLE, *J. Less-Common Metals* **30** (1973) 63.
3. H. KARIMZADEH, PhD thesis, University of Manchester (1985).
4. K.I. GRADWELL, PhD thesis, University of Manchester (1972).
5. G. OMORI, S. MATSUO and H. ASADA, *Trans, JIM* **16** (1975) 247.
6. G. OMORI, *Trans. Nat. Res. Insti. Metals* **21** (4) (1979) 38.
7. W.B. PEARSON, "Pearson's Handbook of Crystallographic Data for Intermetallic Phases", edited by P. Villars and L.O. Calvert, 2nd edn. (ASM International, Materials Park, OH, 1991) p. 2269.
8. W. HUME-ROTHERY, R.E. SMALLMAN and C.W. HAWORTH, "The Structure of Metals and Alloys", London, Monograph and Report Series, No. 1 (Institute of Metals, London, 1969) pp. 336-40.
9. A.A. NAYEB-HASHEMI and J.B. CLARK, *Bull. Alloy Phase Diagrams* **9**(2) (1988) 162.

Received 19 September 1994
and accepted 11 May 1995